Sensors and Materials, Vol. 36, No. 8 (2024) 3445–3452
MYU Tokyo

S & M 3743

Noncontact Temperature Measurement of Metal Surfaces Using Reflected Laser Beam

Taichi Murakami,[1] Masaki Shimofuri,[2] Toshiyuki Tsuchiya,[2] and Shugo Miyake[1*]

[1]Setsunan University, 17-8 Ikedanakamachi, Neyagawa-shi, Osaka 572-8508, Japan
[2]Kyoto University, Kyotodaigakukatsura, Nishikyo-ku, Kyoto 615-8246, Japan

(Received May 31, 2024; accepted June 24, 2024)

Keywords: thermoreflectance, microscale spatial resolution, metal thin film, modulation-free heating

A temperature measurement system with a reflected laser beam that does not require temperature modulation was developed for the thermal design of electronic devices. The system combines a balanced photodetector and lock-in amplifier to make reflectance change measurements possible with an extremely high signal-to-noise ratio. First, to evaluate the accuracy of the reflectance change measurement, the reflectance change of a Ni thin film temperature-controlled by a heater and thermocouples was measured as a function of temperature change. To evaluate the accuracy of the temperature change measurement, the reflectance change was measured by heating a Ni thin film that imitated the wiring pattern of an electronic circuit. The experimental results showed that the standard deviation of the ratio of reflectance change from the reference reflectance was $<1.00 \times 10^{-5}$ at a constant temperature. Moreover, the error margin of the calculated temperature change was ±1.0% for a change of 22 °C or more from the reference temperature, and the performance was sufficient for the estimation of local temperature.

1. Introduction

The electronics industry, which is central to a supersmart society, has shown remarkable development in recent years. Electronic devices are becoming more sophisticated and multifunctional. It is extremely important to ensure the reliability of electronic devices, such as smartphones, which have become indispensable to people in their daily lives. However, the thermal management of the heat generated during operation is becoming increasingly difficult as components and circuits are integrated more densely. Therefore, to design optimal thermal management at the microscale and nanoscale levels, a technology that can measure temperatures in a small area easily and accurately is required. Temperature measurement technologies with microscale spatial resolutions that are currently in practical use include thermocouples, radiation thermometers, and Raman spectroscopy.[1–3] Among them, thermoreflectance (TR) imaging, which utilizes the temperature dependence of the reflectance of metal and semiconductor surfaces, has attracted considerable attention. TR imaging measures mainly visible light, which

*Corresponding author: e-mail: shugo.miyake@setsunan.ac.jp
https://doi.org/10.18494/SAM5165

ISSN 0914-4935
https://myukk.org/

is noncontact and has a higher spatial resolution than that of radiation thermometers using infrared rays. On the other hand, since Raman scattering does not occur on pure metals, this TR method is suitable for temperature measurement. Equation (1) shows the relational equation of the TR method.

$$\Delta R/R = C_{TR}\Delta T \tag{1}$$

Here, R is the reflectance at the reference temperature, ΔR is the reflectance change from R, C_{TR} (1/°C) is the TR coefficient and is a material specific value, ΔT is the temperature change from the reference temperature, and ΔT can be obtained by dividing the measured $\Delta R/R$ by C_{TR}. C_{TR} depends on the wavelength of the illuminating light and material. The magnitude of C_{TR} for metals and semiconductors ranges from 10^{-3} to 10^{-5}. Therefore, the reflectance change ($\Delta R/R$) that occurs in response to the temperature change (ΔT) is very small. Because C_{TR} is constant from room temperature to approximately 100 °C, $\Delta R/R$ is linear with respect to ΔT. This facilitates the temperature calibration of systems based on the TR method.

TR imaging can be broadly classified into two types. The first type uses LEDs as the light source.[4–13] TR imaging is characterized by the formation of an image on a CCD element and the acquisition of a two-dimensional image at a time without the need for stage scanning. By increasing the magnification of the imaging lens, measurements can be performed with a high spatial resolution. White LEDs can be used to narrow the measurement wavelength to those with a high C_{TR}.[4–9] Therefore, preparing a separate light source is unnecessary, making it easy to perform high-sensitivity measurements in response to sample changes. However, the signal-to-noise ratio of the CCD is low, and there is a quantization limit consisting of a finite number of bits.[10] Therefore, it is necessary to repeat the measurements for several minutes to several hours and perform the averaging process. The second type uses a laser as the light source.[14–19] A laser beam is monochromatic and coherent, and its spatial resolution is in the sub-micrometer range. Two-dimensional images can be obtained by scanning the sample stage or laser spot. The temperature modulation of the sample and the lock-in detection of the intensity-modulated reflected light make it possible to measure $\Delta R/R$ versus ΔT with a high signal-to-noise ratio. TR measurement by temperature modulation is effective for devices with switching operation using such components as transistors. However, this is not applicable to devices or circuits with DC operation. In addition, when the heat transfer pattern from the heat source to the surroundings of a device is being studied, nonstationary temperature modulation complicates the analysis if nonlinear effects, such as thermal radiation, are included.

In this study, a temperature measurement system that uses a reflected laser beam that does not require temperature modulation was developed. First, to evaluate the $\Delta R/R$ measurement accuracy of the developed system, the change in reflectance in a Ni thin film with known C_{TR} was measured. Moreover, to evaluate the ΔT measurement accuracy of the system, a Ni thin film that imitates the wiring pattern of an electronic circuit was heated by an electric current, and the temperature increase of the surface was measured.

2. Experimental Setup

Figure 1 shows the system developed in this study. The optical system is covered with an insulated box and an optical surface plate. The temperature is kept at 22 ± 0.3 °C using a precision air conditioner. The light source is a single-mode fiber-coupled semiconductor laser with a wavelength of 642 nm, which is a large wavelength for visible light. The laser beam is collimated by a collimator at the fiber exit end and emitted into free space. An objective lens—10×, working distance (*WD*) = 5.5 mm, and numerical aperture (*NA*) = 0.25—focuses the laser beam onto the sample surface on the stage. The focus shift is affected by thermal expansion during heating; however, this is avoided by using a low-NA objective lens in the developed optical system. To do so, the spot diameter (spatial resolution) measured by the knife-edge method is 10 μm. The laser intensity used to illuminate the sample is 0.5 mW. Each laser beam, before and after sample illumination, is bifurcated using a nonpolarizing beam splitter and injected into a balanced photodetector (PD; Newport Model 2307). The balanced PD consists of two photodiodes and a differential amplifier circuit. The use of a differential circuit eliminates several percentage points of the source noise, which is much larger than that of C_{TR}. The voltage balance of the differential circuit is adjusted using a neutral density (*ND*) filter inserted on the PD1 side. The laser intensity is modulated by the output signal of the function generator. The modulation frequency is sinusoidal at 1 kHz. Lock-in detection at the modulation frequency using a lock-in amplifier (Stanford Research Systems SR830) is used to measure minute reflectance changes with a high precision. The combination of a balanced PD and lock-in amplifier makes measurement possible with a high signal-to-noise ratio.

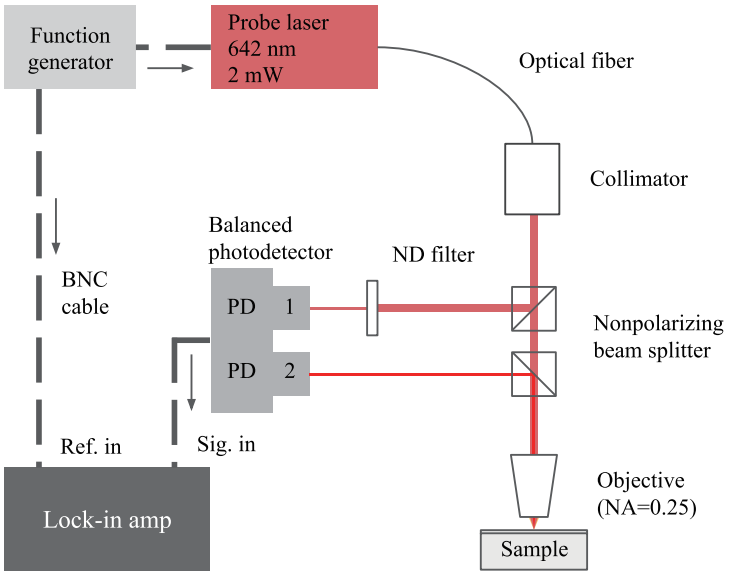

Fig. 1. (Color online) Temperature measurement system based on TR method.

Figure 2 shows the temperature control system for the Ni thin film surface. In this experiment, Ni, which has a relatively small C_{TR}, was used as the sample for measurement, and a Ni thin film with a thickness of 100 nm was deposited on a 10 mm^2, 1-mm-thick soda-lime glass substrate using a DC sputtering system. The deposition conditions were as follows: power input of 50 W, initial exhaust gas pressure of 5.0×10^{-4} Pa, argon gas pressure of 0.2 Pa, distance of 100 mm between target substrates, deposition time of 20 min, and substrate temperature of room temperature. An alumina heater was attached to the back of the glass substrate for heating. A Type K thermocouple was mounted approximately 2 mm from the measurement point. The in-plane temperature of the Ni thin film was assumed to be constant because of the heat capacity of the glass substrate. In addition, 10-mm-thick quartz glass was inserted between the substrate and the sample stage to suppress thermal expansion. To confirm the repeatability of $\Delta R/R$ measurement, a heating and cooling cycle was performed from room temperature to 100 °C, and $\Delta R/R$ during the cycle was measured. Heating and cooling were performed every 20 °C from room temperature. The temperature was maintained for 300 s, and the temperature increase and decrease were controlled at intervals of 60 s. The measurements were performed at an ambient temperature of 22 °C under atmospheric pressure. The sampling rate of the detected laser intensity was set to 1 s.

The Ni wiring pattern film shown in Fig. 3 was subjected to current heating. The Ni thin film was processed into a thin wire 1 mm wide and 10 mm long on a glass substrate. As the line width changes, the volume of the thin wire changes, and thus the heat capacity also changes. For narrower line widths, such as a few μm, the transient temperature rise for instantaneous heating is steeper because of the smaller heat capacity. Moreover, the measured reflectance change is more sensitive to the displacement of the sample or laser optical axis. The measurement point was one point at the center of the thin wire. Voltage was applied to the electrode pads at both ends of the thin wire for current heating. The temperature increase was then determined from the C_{TR} of the Ni thin film. After the voltage was applied, $\Delta R/R$ was measured at 100 points after thermal equilibrium was reached.

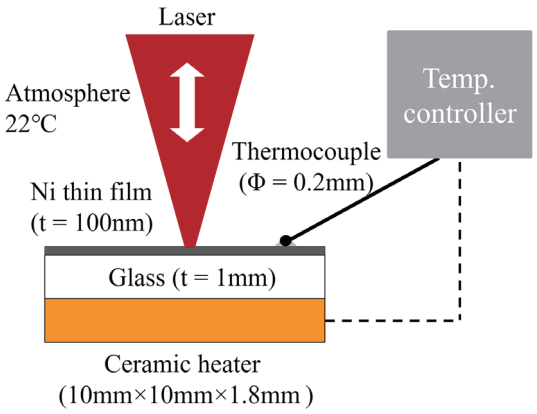

Fig. 2. (Color online) Temperature control system for Ni thin film surface.

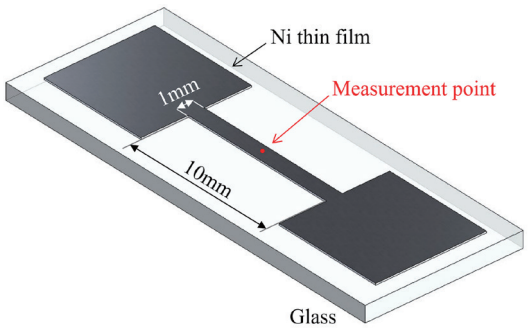

Fig. 3. (Color online) Wiring pattern of Ni thin film.

3. Results and Discussion

Figure 4 shows the results of reflectance change measurements for the heating and cooling cycles. The left vertical axis shows the measured $\Delta R/R$. $\Delta R/R$ is plotted as open circles. The right vertical axis represents the Ni thin film surface temperature. This temperature is indicated by a solid line. The horizontal axis represents the measurement time. $\Delta R/R$ decreased consistently with increasing temperature and increased consistently with decreasing temperature. A sharp peak occurred at approximately 1800 s for both temperature and $\Delta R/R$. This was because the proportional-integral-derivative temperature control had ended. A gradual curve of spontaneous cooling from 40 °C to room temperature was observed. At the end of the measurement, there was not sufficient time for the Ni thin film to cool to room temperature+1 °C. The standard deviation of $\Delta R/R$ measured during 300 s at each set temperature was $<1.00 \times 10^{-5}$. The surface temperature accuracy of the Ni thin film measured by a thermocouple was approximately 0.1 °C. Figure 5(a) shows a plot of the average $\Delta R/R$ at each temperature setting in Fig. 4. The vertical axis represents $\Delta R/R$

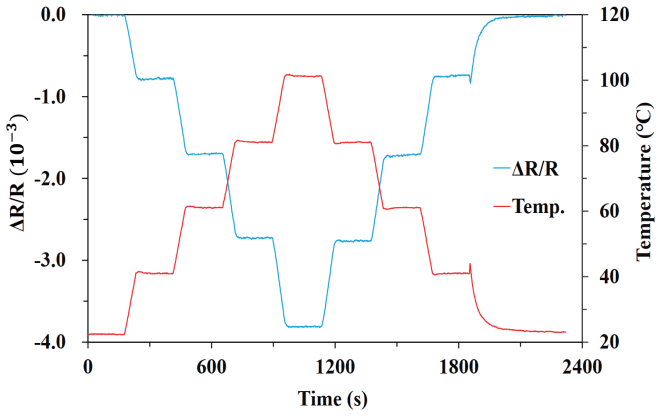

Fig. 4. (Color online) Measured $\Delta R/R$ during heating and cooling cycles.

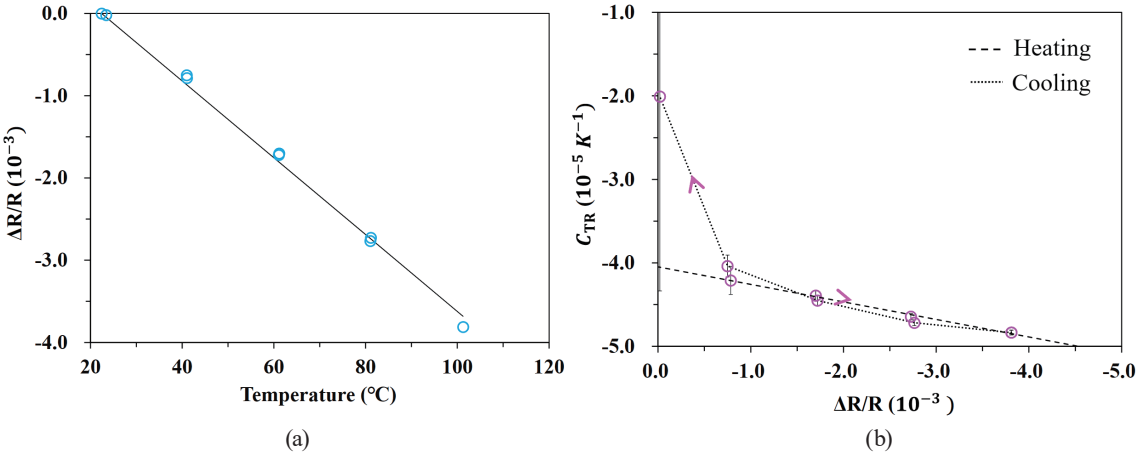

Fig. 5. (Color online) (a) Reflectance change for each set temperature and (b) C_{TR} calculated for each $\Delta R/R$.

and the horizontal axis represents the Ni thin film surface temperature. The dashed line is the regression line of $\Delta R/R$ to temperature. The residual standard deviation was relatively large at 8.09×10^{-5}. Hysteresis in $\Delta R/R$ was considered to have occurred before and after heating and cooling. It was reported previously that C_{TR} varies greatly depending on the presence of an oxide film on the surface.[20,21] In this experiment, the Ni thin film was heated and cooled while being exposed to atmospheric pressure; thus, an oxide film may have grown. The oxide film may weaken the linearity of $\Delta R/R$ with respect to the temperature change in the Ni thin film.

Figure 5(b) shows C_{TR} calculated by dividing $\Delta R/R$ in Fig. 5(a) by the temperature change ΔT of the Ni thin film relative to the reference temperature (room temperature). The number of plots was reduced from 9 to 8 in Fig. 5(a) because room temperature during heating was used as the reference temperature. The dashed line shows the regression line of C_{TR} to $\Delta R/R$ for the heating process from room temperature to 100 °C. The residual standard deviation is very small at 2.17×10^{-7} [1/°C], and the accuracy of the regression line is good. Dashed lines with shorter intervals indicate C_{TR} for the cooling process from 100 °C to room temperature. All C_{TR} values are negative on the order of 10^{-5}, which is consistent with literature values.[22,23] C_{TR} decreases with increasing temperature; however, the values differed between the above processes. In the cooling process, C_{TR} increased as $\Delta R/R$ approached 0. In particular, C_{TR} at $\Delta R/R = -1.97 \times 10^{-5}$ was less than half that at $\Delta R/R = -0.75 \times 10^{-3}$. In addition, the error was extremely large, ±116%. The errors in C_{TR} for heating processes were ±4% for $\Delta R/R = -0.78 \times 10^{-3}$, ±1.4% for $\Delta R/R = -1.70 \times 10^{-3}$, ±0.8% for $\Delta R/R = -2.73 \times 10^{-3}$, and ±0.6% for $\Delta R/R = -3.81 \times 10^{-3}$. Therefore, to achieve an error in C_{TR} within ±1%, $\Delta R/R$ must decrease by more than -2.73×10^{-3}.

Figure 6(a) shows the $\Delta R/R$ measurement results during the current heating of the Ni wiring film. The vertical axis represents $\Delta R/R$, and the horizontal axis represents the square of applied voltage, V^2. The dashed line shows the regression line of $\Delta R/R$ to the square of applied voltage. The residual standard deviation was 1.43×10^{-5}. $\Delta R/R$ decreased

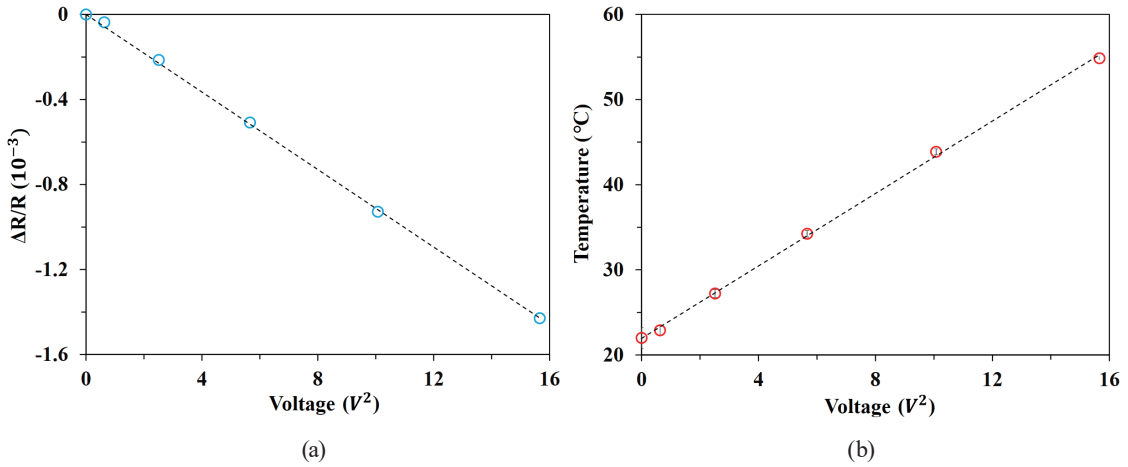

(a) (b)

Fig. 6. (Color online) (a) Reflectance change measured during current heating and (b) temperature change calculated using C_{TR}.

proportionally to V^2, which can be regarded as the amount of heating. The minimum $\Delta R/R$ was -1.4×10^{-3}. This current heating of the Ni thin film was the only heating process; therefore, the C_{TR} value calculated using the high-accuracy regression line in Fig. 5(b) was used. Figure 6(b) shows $\Delta R/R$ in Fig. 6(a) divided by C_{TR} and converted to temperature. The vertical axis represents the temperature, and the horizontal axis represents V^2. The dashed line is the regression line of temperature to V^2. The residual standard deviation was 0.39 °C. Temperature increases of as much as 54.86 °C were observed. The errors in temperature calculated from the accuracy of $\Delta R/R$ and C_{TR} were ±5.3% for T = 22.90 °C, ±2.2% for T = 27.22 °C, ±1.3% for T = 34.24 °C, ±0.9% for T = 43.87 °C, and ±0.6% for T = 54.86 °C. Therefore, temperature can be determined from the error within ±1% for ΔT of more than 22 °C. As opposed to 1 point temperature measurement, when using this method to obtain temperature mapping, care should be taken to avoid focus shift during laser scanning. The in-plane focus shift is caused by the flatness of the sample and the accuracy of the sample stage movement. Moreover. the temperature mapping of different material surfaces should be calculated from the measured reflectance change to the temperature change using material-specific C_{TR}.

4. Conclusion

A temperature measurement system that uses a reflected laser beam that does not require temperature modulation was developed. First, to evaluate the accuracy of the measurement reflectance change $\Delta R/R$, a Ni thin film with a known TR coefficient C_{TR} was subjected to a temperature-controlled heating/cooling cycle, and $\Delta R/R$ was measured with respect to the surface temperature change ΔT. The standard deviation of $\Delta R/R$ measured during 300 s at each set constant temperature was $<1.00 \times 10^{-5}$. The residual standard deviation of the regression line of $\Delta R/R$ upon temperature change was as large as 8.09×10^{-5}, indicating low linearity. The C_{TR} value obtained by dividing $\Delta R/R$ by ΔT was negative, and its order was consistent with the values reported in the literature. The error in C_{TR} became smaller as $\Delta R/R$ increased, and, when $\Delta R/R$ was smaller than -2.73×10^{-3}, the error was less than ±1.0%. Moreover, to evaluate the accuracy of ΔT measurement, $\Delta R/R$ was measured against ΔT by applying electric current heating to a Ni thin film that imitated the wiring pattern of an electronic circuit. As a result, $\Delta R/R$ decreased proportionally to the square of the applied voltage, which can be regarded as the amount of heating. In the current heating experiment, only heating was performed. Therefore, C_{TR} was obtained using a high-precision regression line obtained during heating in the experiment. ΔT was calculated by dividing the measured $\Delta R/R$ by C_{TR}, and the error was less than ±1.0% when ΔT was 22 °C or higher.

Acknowledgments

Part of this research was supported by a JST Grant-in-Aid for Scientific Research (Project Nos. 21H01261 and 24H00284).

References

1 C. Cengiz, M. Azarifar, and M. Arik: Micromachines **13** (2022) 2. https://doi.org/10.3390/mi13101615
2 L. Dupont, Y. Avenas, and P. O. Jeannin: IEEE Trans. Ind. Appl. **49** (2013) 1599. https://doi.org/10.1364/OE.27.007945
3 B. Davaji, J. E. Richie, and C. H. Lee: Sci. Rep. **9** (2019) 6546. https://doi.org/10.1038/s41598-019-42999-w
4 D. U. Kim, K. S. Park, C. B. Jeong, G. H. Kim, and K. S. Chang: Opt. Express **24** (2016) 13906. https://doi.org/10.1364/OE.24.013906
5 H. Zhang, S. Wen, and A. Bhaskar: Appl. Phys. Lett. **114** (2019) 151902. https://doi.org/10.1063/1.5087011
6 B. Vermeersch, J. Bahk, J. Chirstofferson, and A. Shakouri: J. Appl. Phys **113** (2013) 1. https://doi.org/10.1063/1.4794166
7 D. Pier´sci´nska: J. Phys. D: Appl. Phys. **51** (2018) 013001. https://doi.org/10.1088/1361-6463/aa9812
8 M. Farzaneh, K. Maize, D. Lüerßen, J. A. Summers, P. M. Mayer, P. E. Raad, K. P. Pipe, A. Shakouri, R. J. Ram, and J. A. Hudings: J. Phys. D: Appl. Phys. **42** (2009) 1. https://doi.org/10.1088/0022-3727/42/14/143001
9 Y. Gao, J. Jin, Y. Ruan, Y. Gao, L. Zhu, Z. Guo, Y. Lin, Z. Chen, and Y. Lu: Opt. Express **27** (2019) 7945.
10 R. Mckenna, D. Mickus, S. Naimi, C. Murphy, M. Mcdermott, S. Corbett, D. Mccloskey, and J. F. Donegan: OSA Continuum **4** (2021) 1271. https://doi.org/10.1364/OSAC.422429
11 T. Zhu, D. H. Olson, P. E. Hopkins, and M. Zebarjadi: Rev. Sci. Instrum. **91** (2020) 113701. https://doi.org/10.1063/5.0024476
12 Y. Zhang, J. Chirstofferson, A. Shakouri, D. Li, A. Majumdar, Y. Wu, R. Fan, and P. Yang: IEEE Trans. Nanotechnol. (2006) 67. https://doi.org/10.1109/TNANO.2005.861769
13 Y. Sugihara, R. Uemura, K. Tamai, R. Kuriyama, and K. Tatsumi: The 33rd Int. Symp. Transport Phenomena (2023) 67–74.
14 D. U. Kim, C. B. Jeong, J. D. Kim, K. Lee, H. Hur, K. Nam, G. H. Kim, and K. S. Chang: Sensors **17** (2017) 2774. https://doi.org/10.3390/s17122774
15 P. M. Mayer, D. Lüerßen, R. J. Ram, and J. A. Hudgings: J. Opt. Soc. Am. A **24** (2007) 1156.
16 S. Dilhaire, S. Grauby, and W. Claeys: Appl. Phys. Lett. **84** (2004) 822. https://doi.org/101063/1.1645326
17 D. Pier´sci´nska, A. Kozlowska, K. Pier´sci´nski, M. Bugajsk, J. W. Tomm, M. Ziegler, and F. Weik: J. Mater. Sci. Mater. Electron. **19** (2008) S150–S154. https://doi.org/10.1007/s10854-008-9643-z
18 P.-L. Komarov, M. G. Burzo, and P.-E. Raad: Proc. 12th THERMINIC (2006) 12–17.
19 M. G. Burzo, P. L. Komarov, and P. E. Raad: IEEE Trans. Compon. Packag. Manuf. Technol. **28** (2005) 637–643. https://doi.org/10.1109/TCAPT.2005.859738
20 C. Shi, X. Wang, Q. Zheng, J. Maroske, and D. Thompson: Opt. Express **32** (2024) 1003. https://doi.org/10.1364/OE.511938
21 T. Favaloro, J.-H. Bahk, and A. Shakouri: Rev. Sci. Instrum. **86** (2015) 024903. https://doi.org/10.1063/1.4907354
22 B. Meng, Y. Ma, X. Wang, and C. Yuan: J. Appl. Phys. **134** (2023) 115102. https://doi.org/10.1063/5.0164110
23 J. Hanus, J. Feinleib, and W. Scouler: Phys. Rev. Lett. **19** (1967) 16. https://doi.org/10.1103/PhysRevLett.19.16